Proceedings of the 9th U.S. National and 10th Canadian Conference on Earthquake Engineering
Compte Rendu de la 9ième Conférence Nationale Américaine et
10ième Conférence Canadienne de Génie Parasismique
July 25-29, 2010, Toronto, Ontario, Canada • Paper No 848

NONLINEAR STATIC SEISMIC ANALYSIS AND ITS VALIDATION USING DAMAGE DATA FROM REINFORCED-CONCRETE SCHOOL BUILDINGS

Y. H. Tu[1], T. W. Liu[2], L. C. Ao[3], and P. L. Yeh[4]

ABSTRACT

This paper introduces a simplified nonlinear static seismic analysis method that consists of a simplified procedure for push-over analysis and a procedure modified from the capacity spectrum method from ATC-40. The simplified push-over curve is obtained on the basis of assumptions for failing behavior, such as strong-beam–weak-column behavior, which is commonly observed in low-rise reinforced-concrete buildings. This limits the usage of the method but allows other merits in analysis, such as abbreviating the calculation and allowing for strength degradation or detailed consideration for the capacity curve of members. Data of 31 school buildings from a damage databank were employed to validate the method. The analytical seismic capacity was compared to the earthquake intensity that each building experienced. The proposed method produced generally conservative results with no overestimates for the seismic capacity of the buildings.

Introduction

Damage data of past earthquakes are especially valuable for seismic research, including seismic assessment, damage evaluation, and hazard mitigation. Since the Taiwan midlands were struck by the Chi-Chi earthquake in 1999, there have been numerous studies on the damage to building structures, most of these studies were supported by the National Center for Research on Earthquake Engineering (NCREE), Taiwan. A seismic database with a geographical information system (GIS) was also established (Hsieh et al. 2002) by integrating damage data of schools and public buildings obtained from the NCREE and apartment houses, whose data was obtained from the Taiwan Construction Research Institute. This database is very useful for hazard mitigation in a large region. However, the lack of structural details in the database limits its applicability, and thus, it cannot be used for research involving seismic assessment of individual buildings. Therefore, many years after the Chi-Chi earthquake, another databank containing more detailed data was established (Tu et al. 2009). Typical low-rise reinforced-concrete (RC) school buildings in Nantou County were chosen as subjects because of their similar structural systems and the serious damage

[1]Assistant Professor, Department of Architecture, National Cheng Kung University, Tainan 701, Taiwan
[2]Research Assistant, National Center for Research on Earthquake Engineering, Taipei 106, Taiwan
[3]Graduate Student, Department of Architecture, National Cheng Kung University, Tainan 701, Taiwan
[4]Master, Department of Architecture, National Cheng Kung University, Tainan 701, Taiwan

they suffered in the earthquake. The databank could not only be employed in developing the motion-damage relationship but was also useful for validating and improving detailed seismic assessment methods. This paper presents a nonlinear static seismic assessment procedure that follows the capacity spectrum method (CSM) from the ATC-40 report (ATC 1996). Data of selected buildings from the databank were compared with analytical results to validate this method.

Brief Introduction of the Analytical Method

Simplified push-over analysis (SPOA) is a nonlinear static seismic assessment method developed for low-rise RC buildings. It consists of two main parts: (1) obtaining a capacity/push-over curve and (2) finding the corresponding demand peak ground acceleration (PGA) for the capacity curve. To abridge the time for iterative structural analysis, the first part is performed with a simplified procedure. The second part basically follows CSM with some modifications.

Basic Assumption and the Simplified Procedure for Obtaining Push-Over Curve

The simplified procedure is only sustainable for buildings that agree with its basic assumptions. The procedure assumes that the structure fails through the strong-beam–weak-column behavior commonly observed in typical low-rise RC buildings. This behavior occurs when beams and slabs in RC buildings are cast in one piece. The beams become strengthened and more rigid than expected, which results in prior failure of the vertical members. With relatively rigid beams, the building deforms like a shear building, as illustrated in Fig. 1. In this case, the lateral capacity of each storey can be considered as the sum of the contributions of every vertical member in the storey. In order to evaluate the lateral force contribution of vertical members, the capacity curve of each member is needed. The member capacity curves can be defined analytically or obtained from structural experiments, as described on the left side of Fig. 2. Since all of the vertical members are connected to the same rigid slab, the lateral displacement of every member is considered identical to the storey drift. Therefore, storey shear can be obtained by simply superposing the lateral force in every vertical member at a given drift, as shown on the right side of Fig. 2. The concept originates from the seismic evaluation standard for RC buildings in Japan (MLIT 2001). Figure 2 shows that when a group of members fails, strength degradation or negative stiffness is exhibited in the storey force-drift curve. This is usually difficult to simulate in regular structural analysis. The procedure can also exhibit the failure sequence of members clearly. However, this assumption neglects failure in beams.

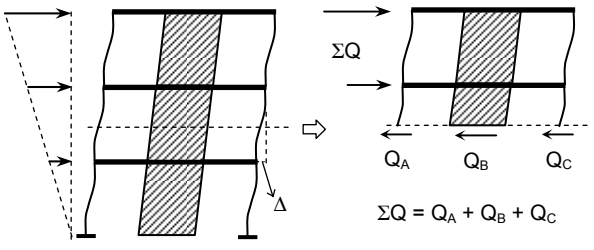

Figure 1. Strong-beam-weak-column behavior

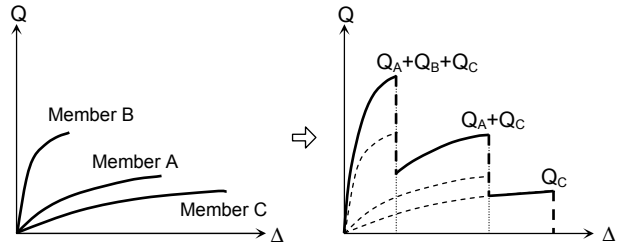

Figure 2. Simplified procedure for storey force-drift curves

The push-over curve, defined as the relationship between base shear and roof displacement, is also obtained with a simplified procedure. The ATC-40 report suggests that the lateral force distribution can be considered as a reverse triangle, as shown in Fig. 3. By comparing the base shear corresponding to the maximum shear in each storey, the storey that governs the minimum base shear is determined as the failure control storey. The procedure also assumes that the lateral deformation is governed by the fundamental mode, as shown in Fig. 4. Roof displacement is therefore the summation of every storey drift at a given base shear.

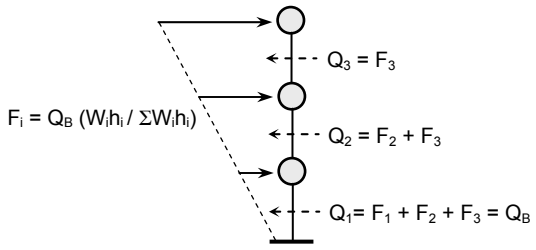

Figure 3. Relationship between storey and base shears

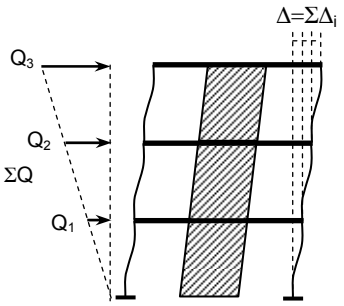

Figure 4. Calculation of roof displacement

Capacity Spectrum and Corresponding PGA

The push-over curve was converted into the capacity spectrum in acceleration-displacement response spectra (ADRS) format as suggested by ATC-40. In the original CSM, a performance point P is defined as the intersection of the capacity and demand spectra, as shown in Fig. 5(a). The demand spectrum is reduced from an elastic demand spectrum according to the equivalent damping ratio β_{eq}, which is derived from the position of the intersection point. In this procedure, only one performance point can be obtained for each given demand spectrum, and iterative calculation is needed.

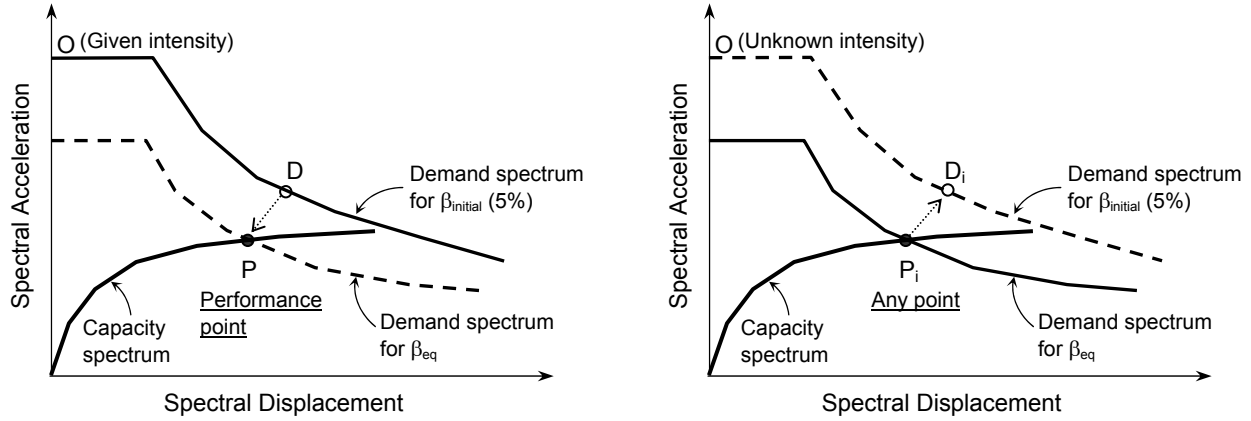

(a) CSM (b) SPOA

Figure 5. Comparison between CSM and SPOA

SPOA uses the procedure in reverse. Any point P_i on the capacity spectrum is a given performance point for finding the corresponding demand spectrum. The corresponding demand spectrum is defined as a normalized given spectrum magnified with an unknown intensity ratio S_{A0}. Since point P_i is also on the demand spectrum for β_{eq}, a corresponding point D_i on the elastic demand spectrum can be found by dividing the spectral acceleration of P_i with the reduction coefficient at β_{eq}. The intensity ratio of elastic demand spectrum can then be determined, as shown in Eq. 1.

$$S_{A0} = \frac{S_A}{C \times C_D} \tag{1}$$

where S_A is the spectral acceleration of P_i. C_D is the reduction coefficient corresponding to β_{eq}, and was inspired by Kawashima and Aizawa (1986). C is the normalized demand spectral acceleration corresponding to the equivalent period T_{eq} of P_i, which is defined by the shape of the demand spectrum. The equivalent period and damping are calculated according to ATC-40, as shown in Eqs. 2 and 3. S_D is the spectral acceleration of P_i. β_0 is the hysteretic damping, and κ is an adjustment factor for the hysteretic behavior.

$$T_{eq} = 2\pi\sqrt{\frac{S_D}{S_A \cdot g}} \tag{2}$$

$$\beta_{eq} = 5\% + \kappa \cdot \beta_0 \tag{3}$$

The magnifying ratio for the normalized demand spectrum S_{A0} is actually the PGA of the demand earthquake. Therefore, a corresponding PGA curve can be derived from the entire capacity curve. The collapse point of the structure is defined as (1) where the first member fails by shear or (2) where the base shear of the structure reaches its maximum and decreases to 80% of its value. The PGA corresponding to the collapse point is considered as the ultimate seismic capacity of the structure.

Capacity Curve of Individual Vertical Members

Figures 6 and 7 show the analytical models for capacity curves of RC columns and confined masonry walls that were used in this study. Since there were no RC walls in the school buildings of the databank, the model for RC walls was not included in the validation. The capacity curve for RC columns is defined as a multi-linear model divided by the main damage stages: cracking, yielding, ultimate, and failure. Definitions for force and displacement at each stage are summarized in Table 1 and Eqs. 4–9. Failure mode was determined from the minimum flexural and shear strength. The flexural and shear strength at cracking (Q_{fC} and Q_{sC}) and the ultimate stage (Q_{fU} and Q_{sU}) were calculated according to the provisions of ACI-318 (ACI 2008). As shown in Eq. 4, the displacement of each stage Δ_i is the summation of the

displacements Δ_{fi}, Δ_{si}, and Δ_{ai} caused by flexure, shear, and bond slip, respectively. However, a drift limit of 3% was defined for flexural failure, and Eq. 10 (Elwood 2002) defines the shear failure displacement as the corresponding strength drops to zero. Because of the simplified procedure for the push-over curve, strength degradation after ultimate stage can be defined in the models. The models can also be replaced by more detailed curves or experimental ones.

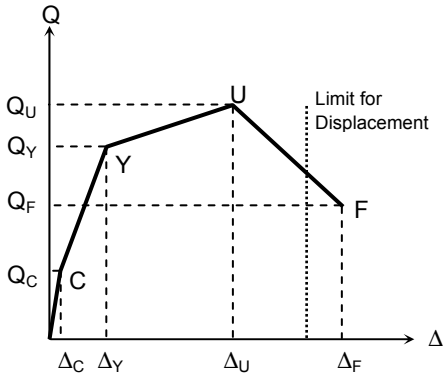

Figure 6. Capacity curve for RC columns

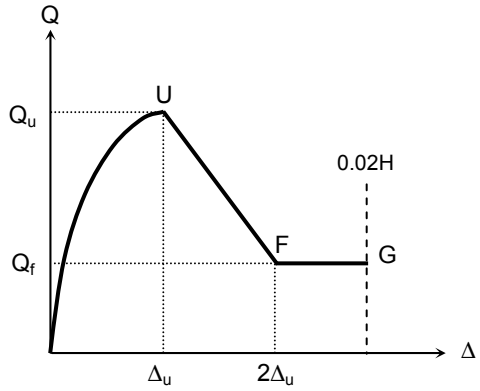

Figure 7. Capacity curve for confined masonry walls

Table 1. Definitions of the force and displacement at each damage point in the capacity curve for RC columns.

	Cracking	**Yielding**	**Ultimate**	**Failure**
Q_i	$Q_C = \min(Q_{fC}, Q_{sC})$	$Q_Y = 0.85Q_U$	$Q_U = \min(Q_{fU}, Q_{sU})$	$Q_F = (Q_C + Q_Y)/2$
Δ_{fi}	Eq. 5 ($C_f = 0.7$)	Eq. 5 ($C_f = I_{eff}/I_{gt}$)	Eq. 5 ($C_f = I_{eff}/I_{gt}$) + Δ_{ph}	Eq. 5 as increment ($C_f = -0.03$)
Δ_{si}	Interpolation from Eqs. 6 and 7 ($C_{sC} = 0.4, C_{sU} = 4.5N\rho_{sh}/(f_c'A_{gt})$)			Eq. 8 ($C_{sF} = -\frac{1}{280}$)
Δ_{ai}	0	Eq. 9 ($C_a = 2.5$)	Eq. 9 ($C_a = 4.5$)	Eq. 9 ($C_a = 4.5$)

$$\Delta_i = \Delta_{fi} + \Delta_{si} + \Delta_{ai} \tag{4}$$

$$\Delta_{fi} = \frac{H^3}{12(C_f \cdot E_c \cdot I_{gt})} \cdot Q_i \tag{5}$$

$$\Delta_{sC0} = \frac{2.4(1+\upsilon)H}{C_{sC} \cdot E_c \cdot A_{gt}} \cdot Q_{sC}, \text{ when } Q_i = Q_{sC}, \text{ where } \upsilon = 0.2 \tag{6}$$

$$\Delta_{sU0} = \frac{2.4(1+\upsilon)H}{C_{sU} \cdot E_c \cdot A_{gt}} \cdot (Q_{sU} - Q_{sC}) + \Delta_{sC0}, \text{ when } Q_i = Q_{sU}, \text{ where } \upsilon = 0.4 \tag{7}$$

$$\Delta_{sF} = \frac{2.4(1+\upsilon)H}{C_{sF} \cdot E_c \cdot A_{gt}} \cdot (Q_F - Q_U) + \Delta_{sU}, \text{ where } \upsilon = 0.5 \quad (8)$$

$$\Delta_{ai} = C_a \cdot \frac{s}{(d - kd)} \cdot H \quad (9)$$

$$\frac{\Delta_f}{H} = \frac{4}{100} \cdot \frac{1 + \tan^2\theta}{\tan\theta + N\left(\frac{S_h}{A_h f_{yh} d_c \tan\theta}\right)} \leq \frac{4}{100}, \text{ where } \theta = 65^\circ \quad (10)$$

Here, I_{eff} is the effective moment of inertia according to ACI-318(2008) provisions. N is the axial load. H is the clear height of the column. d and d_c are the effective depth and depth of the core concrete, respectively. s is the bond slip deformation of steel that is calculated using the equation developed by Sheu (1976). A_h, S_h, ρ_{sh}, and f_{yh} are the area, spacing, steel ratio, and yielding strength of the hoop, respectively. Model details for confined masonry walls can be found in Chen's thesis (2003). The models were validated by comparing the analytical push-over curve with in situ test results for school buildings (Tu et al. 2006).

Content of the Databank

The databank was established following the methodology of ATC-13 (ATC 1985). Every sample in the databank consists of 3 major parts: ground motion intensity, structural properties, and damage condition.

Structural Properties

The original architectural and structural blueprints of the school buildings were kindly provided by the Office of Buildings Management, Nantou County Government and by some of the schools. Blueprints were obtained for only half of the total 188 primary and secondary schools. Most of the blueprints were not complete because of an old policy of the Ministry of Education to construct classrooms in installments. Most of the school buildings had a typical plan and structural system, as shown in Fig. 8; classrooms along a corridor with openings in the longitudinal direction and partition walls in the transverse direction. The plan was usually identical for every storey; thus, generally typical school buildings failed along the longitudinal direction at the base floor. Structural properties including the dimensions of the buildings, number and section of members, steel ratios, and site types were organized from the blueprints and geotechnical soil reports. Material strength could not be determined since most of the damaged buildings were demolished.

Ground Motion Intensity

PGA is used to describe ground motion intensity since it is the most commonly used

index in Taiwan, and it can be directly related to the building code and earthquake intensity scale. Hundreds of triaxial (NS, EW, and vertical axes) accelerometers installed by the Central Weather Bureau recorded the Chi-Chi earthquake motions. Most were installed in schools. PGA at school sites without accelerometers was obtained by interpolation from the 3 nearest accelerometers satisfying the following conditions: (1) distance from each accelerometer to the site is less than 30 km and (2) distances between each accelerometer are as close as possible. Considering that the buildings do not necessarily lie in the NS or EW directions, PGA along the longitudinal and transverse axes of those buildings that can be recognized from the site plan blueprints were also calculated with coordinate rotation.

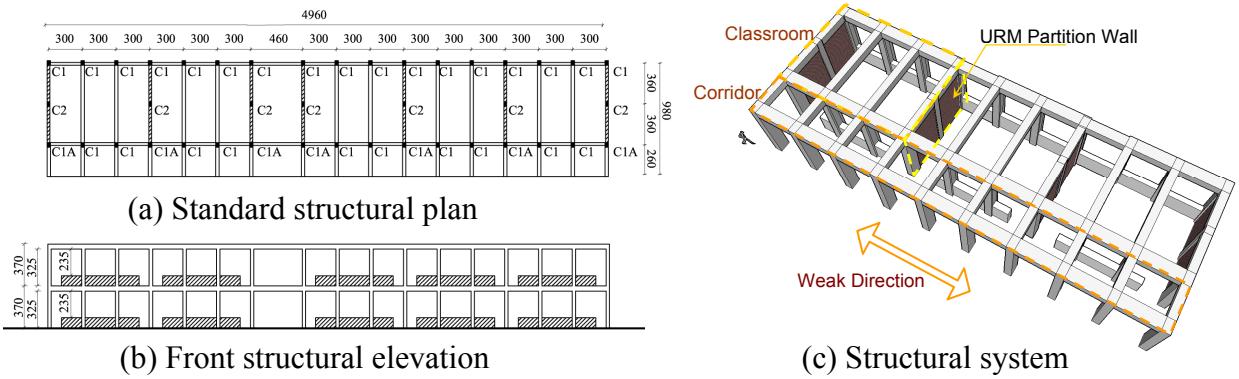

(a) Standard structural plan

(b) Front structural elevation

(c) Structural system

Figure 8. Structural plan, elevation, and system of typical school buildings in Taiwan

Damage Condition

Original damage pictures and records were collected from the existing database and a literature survey. A five-level criterion used in investigating damage from the 1978 Miyagi-Oki and Chi-Chi earthquakes (Table 2) was used to define the damage state qualitatively. Since the amount of damage pictures collected was much less than expected and some were repeated or not identified, inquiries to the school staffs were used as complementary information.

Table 2. Definition of Damage State

Damage State		Description
I	Slight Damage	Columns, shear walls, and secondary walls are slightly or not damaged. (No need for repair)
II	Light Damage	Columns and shear walls are lightly damaged. Shear cracks are found in RC secondary walls or around the staircases. (Building is usable after repair)
III	Moderate Damage	Shear cracks or flexural cracks are found in columns and shear walls. RC secondary walls and non-structural constructions are seriously damaged. (Building should be repaired or retrofitted)
IV	Severe Damage	Steel bars in columns are buckled or exposed due to critical shear or flexural cracking. Serious shear cracking that causes notable strength deterioration is found in shear walls. (Building should be retrofitted or demolished)
V	Collapse	Columns and shear walls are seriously damaged. The building is entirely or partially collapsed.

Comparison between Analytical Result and Databank

Because detailed structural information was needed for nonlinear seismic analysis, only 31 buildings in the databank with relatively complete data were chosen as the subjects. Other information that was not available was assumed. According to common conditions in Taiwan (Hwang et al. 2006), the compressive and yielding strengths of concrete and steel were assumed to be 14.7 MPa (150 kgf/cm^2) and 274 MPa (2800 kgf/cm^2), respectively. Half of the buildings were 2-storey high, 30% were 1-storey high, and the rest were 3-storey high. Since the mean steel ratio was 0.023 and D10 hoops with 25-cm spacing was used for all the buildings in databank, an adjustment factor of $\kappa = 0.33$ was used. The design spectrum from the seismic design code for Taiwan was used as the demand spectrum according to the site type of each school. About half of the buildings were located on class I sites ($\overline{N} > 50$), and the rest were on class II sites ($15 \le \overline{N} \le 50$). In general, both of the push-over curves for the two principal axes of a building were obtained, and the collapse PGA was governed by the weaker one. Since the longitudinal direction is clearly the weak axis for the school buildings, analysis continued only for the longitudinal axis. Figure 9 illustrates the analytical result of the building shown in Figs. 8(a) and (b). In Fig. 9(a), columns were divided into groups according to their section details, axial loading, and clear height. The columns restrained by windowsills at both sides failed first since the restrained portion was deducted from the clear height. The first quadrant of Fig. 9(b) shows that when the first group of columns failed, the base shear dropped, and the building theoretically collapsed. The maximum analytical PGA of the building was 0.32 g. However, buildings were found that survived a 0.38 g earthquake PGA along the longitudinal direction with only moderate damage. The analytical result is apparently conservative for this building.

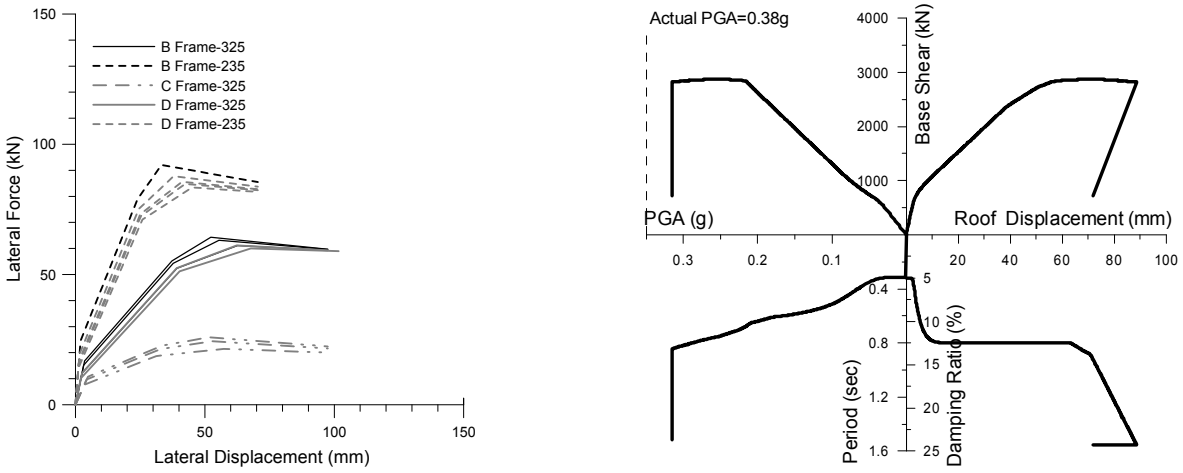

(a) Capacity curves of 1F columns (b) Push-over and PGA curves

Figure 9. Analytical result example

The earthquake PGA along the longitudinal axis was taken as the earthquake PGA (A_E), while the analytical PGA corresponding to the collapse point was defined as the collapse PGA (A_A). Figure 10 shows the relationship between A_A and A_E. Since the damage conditions of

each building were different, the two values are not directly comparable. Therefore, they were classified by the damage state, as shown in the figure. Figure 10(a) shows how the comparison was conducted. For buildings that actually collapsed (Fig. 10(f)), there is no doubt that the earthquake PGA should have exceeded the collapse PGA, so the marks should lie in Zone III. For buildings with only slight, light, or moderate damage (Figs. 10(b)–(d)), A_A should be larger than A_E (Zone I). For buildings severely damaged (Fig. 10(e)), the earthquake PGA should be approximately equal to the collapse PGA, i.e., close to the dotted line (Zone II). Although the boundaries between the different zones and the differences between slight, light, and moderate damage are still unclear and difficult to define, the comparison showed reasonable results. Buildings with lighter damage tended to be distributed in Zone I, while those with heavier damage were in Zones II and III. Except for one outlier, no overestimate was found for severely damaged and collapsed buildings. However, about half of the buildings with slight, light, and moderate damage were clearly underestimated.

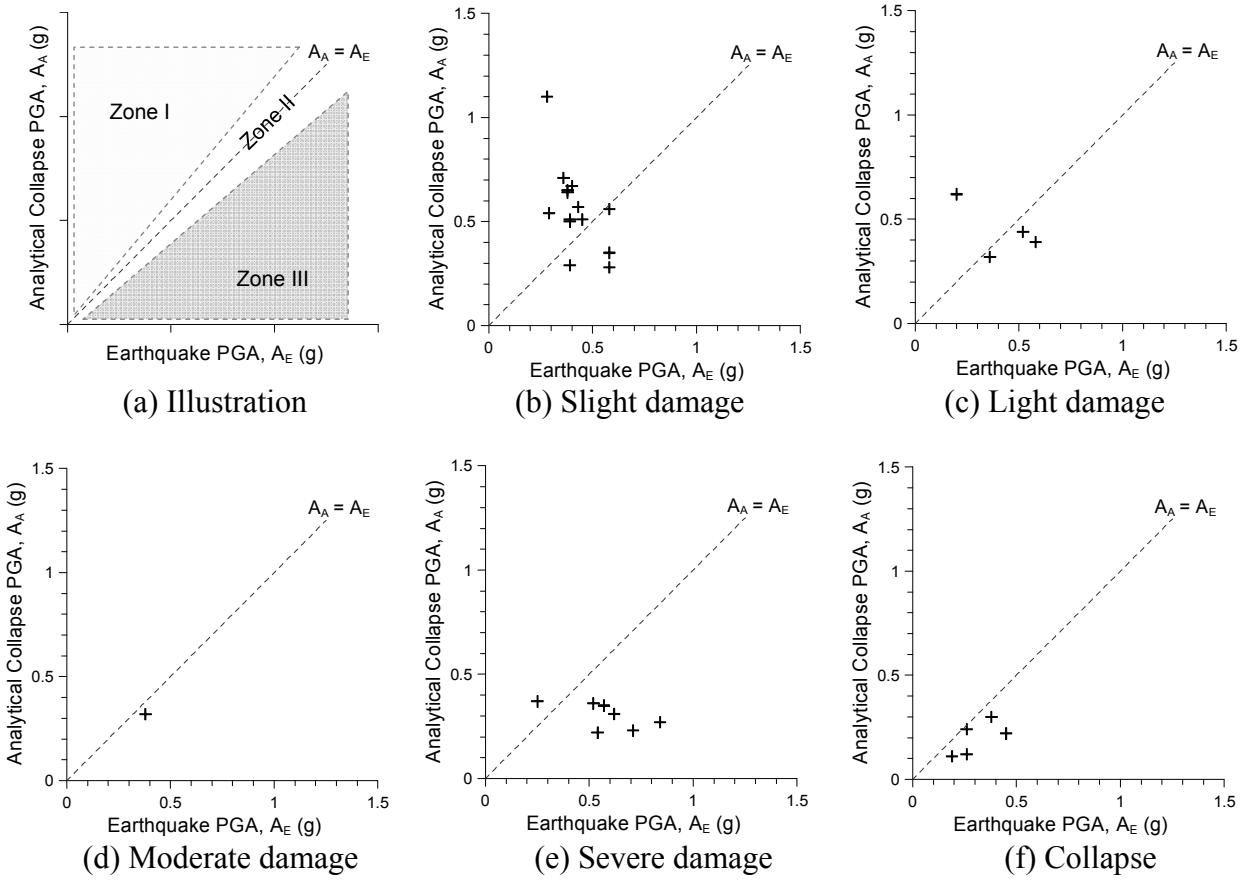

Figure 10. Relationship between analytical collapse PGA and the earthquake PGA

Conclusions

A simplified nonlinear static seismic assessment method is presented in this paper. Based on assumptions for failing behavior, push-over curves can be obtained through simple calculation. The usage of this method is limited to low-rise RC buildings that do not exceed 5

storeys and follow strong-beam–weak-column behavior. The method was validated by comparing 31 buildings that experienced different states of damage in the Chi-Chi earthquake. The analytical results underestimated the seismic capacity for half of the buildings with slight damage, but no overestimate was found in buildings with heavier damage. Although the conservative results may be acceptable when weighing the efficiency against the simplified calculation, further efforts are needed to improve the accuracy of this method.

Acknowledgments

The authors gratefully acknowledge the National Science Council for supporting this research through grant NSC 98-2221-E-006-201.

References

ACI, 2008. *Building Code Requirements for Structural Concrete (ACI318-08) and Commentary*, American Concrete Institute, Farmington Hills, Michigan.

ATC, 1985. Earthquake damage evaluation data for California, *ATC-13 Report*, Applied Technology Council, Redwood City, California.

ATC, 1996. Seismic evaluation and retrofit of concrete buildings, *ATC-40 Report*, Applied Technology Council, Redwood City, California.

Chen, Y. H., 2003. Seismic evaluation of RC buildings infilled with brick walls, *Ph.D. Thesis*, National Cheng Kung University, Tainan, Taiwan. (in Chinese)

Elwood, K., 2002. Shake table tests and analytical studies on the gravity load collapse of reinforced concrete frames, *Ph.D. Thesis*, Department of Civil and Environmental Engineering, University of California, Berkeley.

Hsieh, S. H., P. P. Teng, S. H. Lin, Y. H. Peng, and H. H. Yang, 2002. A study for a seismic assessment operation and establishment of seismic database for damaged buildings – Subproject 2: study on establishment of the seismic database for damaged buildings in the 921 Chi-Chi Earthquake, *Research Report of ABRI*, Architecture and Building Research Institute, Ministry of the Interior, Taipei. (in Chinese)

Hwang, S. J., L. L. Chung, W. Y. Jean, Y. K. Yeh, C. W. Sher, H. C. Chang, Y. K. Wang, and Y. C. Chen, 2006. Implementation planning for seismic evaluation and retrofit of elementary school buildings (II), *NCREE Research Report NCREE-06-004*, National Center for Research on Earthquake Engineering, Taipei. (in Chinese)

Kawashima, K. and K. Aizawa, 1986. Modification of earthquake response spectra with respect to damping ratio, *Proceedings of the third U.S. National Conference on Earthquake Engineering*, South Carolina, pp.1107-1116.

MLIT, 2001. *The Standard for Seismic Evaluation of Existing RC Buildings*, Japan Building Disaster Prevention Association, Tokyo. (in Japanese)

Sheu, M. S., 1976. A gird model for prediction of monotonic and hysteretic behavior of reinforced concrete slab – Column connections transferring moments, *Ph.D. Thesis*, University of Washington, Seattle, Washington.

Tu, Y. H., S. J. Hwang, and T. C. Chiou, 2006. In-site push over tests and seismic assessment on school buildings in Taiwan, *Proceedings of the 4th International Conference on Earthquake Engineering*, October 12-13, Taipei, Taiwan, No. 147.

Tu, Y. H., P. L. Yeh, T. W. Liu, and W. Y. Jean, 2009. Seismic damage evaluation for low-rise RC school buildings in Taiwan, *Proceedings of the 2009 Structures Congress*, April 30-May 2, Austin, Texas, 1347-1356.